Chemical Research in Toxicology

Article

pubs.acs.org/crt

Synthesis and Evaluation of a New Series of Tri-, Di-, and Mono-*N*-alkylcarbamylphloroglucinols as Bulky Inhibitors of Acetylcholinesterase

Ming-Chen Lin,[†] Gin-Zen Lin,[‡] Yu-Fong Shen,[‡,§] Shuo-Yung Jian,[‡] Dean-Kuo Hsieh,[∥] James Lin,[⊥] and Gialih Lin*[,‡,∥]

[†]Division of Internal Medicine, Chung Shan Medical University Hospital, School of Medicine, Chung Shan Medical University, Taichung 402, Taiwan

[‡]Department of Chemistry, National Chung-Hsing University, Taichung 402, Taiwan

[§]Institute of Biological Chemistry and Genomics Research Center, Academia Sinica, Taipei 115, Taiwan

[∥]Department of Applied Chemistry, Chaoyang University of Technology, Taichung 413, Taiwan

[⊥]Department of Aquaculture, National Taiwan Ocean University, Keelung City 202, Taiwan

ABSTRACT: 1,3,5-Tri-*N*-alkylcarbamylphloroglucinols (**1**−**4**) are synthesized as a new series of bulky inhibitors of acetylcholinesterase that may block the catalytic triad, the anionic substrate binding site, and the entrance of the enzyme simultaneously. Among three series of phloroglucinol-derived carbamates, tridentate inhibitors 1,3,5-tri-*N*-alkylcarbamylphloroglucinols (**1**−**4**), bidentate inhibitors 3,5-di-*N*-*n*-alkylcarbamyloxyphenols (**5**−**8**), and monodentate inhibitors 5-*N*-*n*-alkylcarbamyloxyresorcinols (**9**−**12**), tridentate inhibitors **1**−**4** are the most potent inhibitors of mouse acetylcholinesterase. When different *n*-alkylcarbamyl substituents in tridentate inhibitors **1**−**4** are compared, *n*-octylcarbamate **1** is the most potent inhibitor of the enzyme. All inhibitors **1**−**12** are characterized as the pseudo substrate inhibitors of acetylcholinesterase. Thus, tridentate inhibitors **1**−**4** are supposed to be hydrolyzed to bidentate inhibitors **5**−**8** after the enzyme catalysis. Subsequently, bidentate inhibitors **5**−**8** and monodentate inhibitors **9**−**12** are supposed to yield monodentate inhibitors **9**−**12** and phloroglucinol, respectively, after the enzyme catalysis. This means that tridentate inhibitors **1**−**4** may act as long period inhibitors of the enzyme. Therefore, inhibitors **1**−**4** may be considered as a new methodology to develop the long-acting drug for Alzheimer's disease. Automated dockings of inhibitor **1** into the X-ray crystal structure of acetylcholinesterase suggest that the most suitable configuration of inhibitor **1** to the enzyme binding is the (1,3,5)- (*cis*,*trans*,*trans*)-tricarbamate rotamer. The *cis*-carbamyl moiety of this rotamer does not bind into the acetyl group binding site of the enzyme but stretches out itself to the entrance. The other two *trans*-carbmayl moieties of this rotamer bulkily block the tryptophan 86 residue of the enzyme.

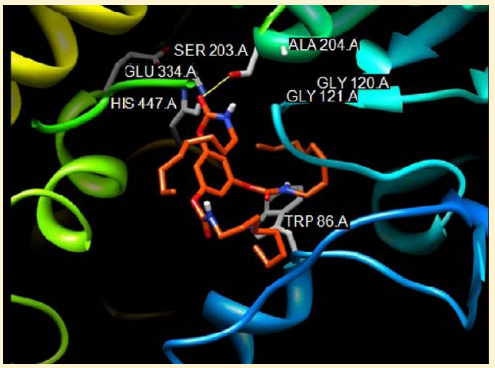

INTRODUCTION

Acetylcholinesterase (AChE, EC 3.1.1.7) belongs to the serine hydrolase family that catalyzes the hydrolysis of acetylcholine (ACh), thus regulating cholinergic neurotransmission.[1−4] Both subtype unselective cholinesterase and AChE-selective inhibitors have been used in Alzheimer's disease to amplify the action of ACh at remaining cholinergic synapses within the Alzheimer's disease brain. The X-ray crystal structures of AChE have revealed that AChE contains a catalytic triad similar to that present in other serine hydrolases. It has also revealed that the catalytic triad Ser-His-Glu is located near the bottom of a deep and narrow gorge about 20 Å in depth.[2−4]

Carbamate inhibitors, such as Alzheimer's disease drug Rivastigmine (Exelon), and aryl carbamates are characterized as the pseudo substrate inhibitors of AChE, butyrylcholinesterase (BChE), cholesterol esterase, and lipase.[3,5−13] In the presence of substrate, the kinetic scheme for pseudo or alternate substrate inhibitions of serine hydrolases by carbamate inhibitors is proposed (Figure 1).[5−15] Therefore, values of K_i and k_2 can be calculated from eq 1.[5] In eq 1, the k_{app} values are

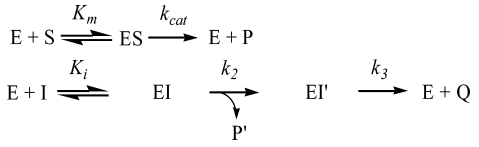

Figure 1. Kinetic scheme for the pseudo substrate inhibition of carbamate inhibitors in the presence of substrate. E, enzyme (AChE); S, substrate (acetylthiocholine); ES, acetylenzyme intermediate; I, inhibitors **1**−**12**; EI, enzyme−inhibitor tetrahedral intermediate; EI′, carbamyl enzyme intermediate; P, product from substrate reaction (thiocholine); P′, product from pseudo substrate reaction (phenols); and Q, the second product (carbamic acids).

Received: March 20, 2012
Published: June 12, 2012

first-order rate constants that are obtained by Hosie's method. The bimolecular rate constant, $k_i = k_2/K_i$, is related to overall inhibitory potency.

$$k_{app} = k_2[I]/\{K_i(1 + [S]/K_m) + [I]\} \quad (1)$$

Recently, dual-site inhibitors of AChE, such as tacrine dimers,[16−20] tacrine-sulfoxide tethers,[21] huperzine B dimers,[22,23] (−)-nor-meptazinol dimers,[24] huperine-tacrine heterodimers,[25] tacrine-indole heterodimers,[26] tacrine-melatonin hybrids,[27] quinazolinimine dimers,[28] tacrine-gallamine hybrids,[29] cymserine,[30] and isosorbide-2-benzyl carbamate-5-salicylate,[31] which may bind to both peripheral anionic substrate binding site (PAS) and anionic substrate binding site (AS) of AChE, have been actively studied by many groups. We have also designed biphenyl-4-acyoxylate-4′-*N*-butylcarbamates,[7] benzene-di-*N*-substituted carbamates,[8] and 1,*n*-alkane-di-*N*-butycarbamates,[9] which may bind to both the PAS and the catalytic triad or esteratic site (ES) of AChE. In this paper, we further design more bulky tridentate inhibitors, 1,3,5-tri-*N*-*n*-alkylcarbamylphloroglucinols (**1**−**4**) (Figure 2) that may bulkily block all of the active site of the

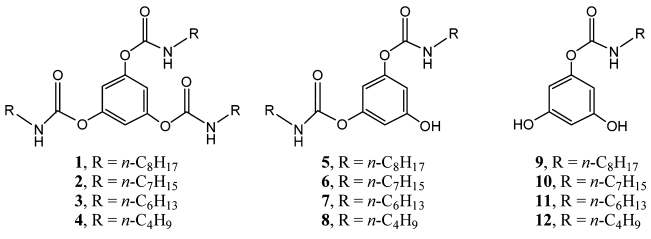

Figure 2. Chemical structures of inhibitors **1**−**12**.

enzyme simultaneously by three carbamyl moieties of the inhibitors.

Bidentate 3,5-di-*N*-*n*-alkylcarbamyloxyphenols (**5**−**8**) (Figure 2) may be produced from the AChE-catalyzed hydrolysis of tridentate **1**−**4** (Figure 3). Subsequently, monodentate 5-*N*-*n*-alkylcarbamyloxyresorcinols (**9**−**12**) (Figure 2) may be from the enzyme-catalyzed hydrolysis of bidentate **5**−**8** (Figure 3). Thus, tridentate inhibitors are designed as long-lived inhibitors of AChE. Therefore, this methodology may be useful to design the long-acting drug for Alzheimer's disease.

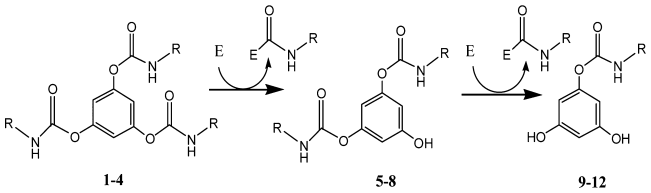

Figure 3. Postulated pathway of the AChE-catalyzed hydrolyses of tridentate inhibitors **1**−**4** followed by hydrolyses of bidentate inhibitors **5**−**8**; E, enzyme.

MATERIALS AND METHODS

Materials. Phloroglucinol (1,3,5-benzene-triol), *n*-alkylisocyanate, triethylamine, and tetrahydrofuran were purchased from Aldrich. Silica gel used in liquid chromatography and thin-layer chromatography plates were obtained from Merck.

Chemistry. 1,3,5-Tri-*N*-alkylcarbamyl phloroglucinols (**1**−**4**), 3,5-di-*N*-alkylcarbamyl-oxyphenols (**5**−**8**), and 5-*N*-alkylcarbamyloxyresorcinols (**9**−**12**) (Figure 2) were synthesized from the condensation of phloroglucinol with 2 equiv of the corresponding *n*-alkylisocyanate and 2 equiv of triethylamine in tetrahydrofuran at 25 °C for 5 h. For example, condensation of phloroglucinol with 2 equiv of octylisocyanate and 2 equiv of triethylamine in tetrahydrofuran at 25 °C for 5 h yielded 1,3,5-tri-*N*-*n*-octylcarbamylphloroglucinol (**1**) (26%), 3,5-di-*N*-*n*-octylcarbamyloxy- phenol (**5**) (12%), and 5-*N*-*n*-octylcarbamyloxyresorcinol (**9**) (19%). These three products were separated and purified by liquid chromatography (silica gel, hexane-ethyl acetate gradient) and characterized by ^{1}H, ^{13}C NMR, and high-resolution mass spectra.

*1,3,5-Tri-N-n-octylcarbamylphloroglucinol (**1**).* ^{1}H NMR ($CDCl_3$, 400 MHz, δ): 0.88 (t, J = 7 Hz, 9H, ω-CH_3), 1.28−1.35 (m, 30H, γ- to ω-1-CH_2), 1.50 (m, 6H, β-CH_2), 3.20 (dt, J = 6.4 and 13.6 Hz, 6H, α-CH_2), 5.29 (t, J = 5.6 Hz, 3H, N*H*), and 6.82 (s, 3H, benzene-*H*). ^{13}C NMR ($CDCl_3$, 100 MHz, assignment from DEPT experiments, δ): 14.0 (ω-CH_3), 22.5, 26.7, 29.1, 29.1, 29.6 (γ- to ω-1-CH_2), 31.7 (β-CH_2), 41.2 (α-CH_2), 111.8 (*C*-2, *C*-4, and *C*-6 of benzene ring), 151.4 (*C*-1, *C*-3, and *C*-5 of benzene ring), and 153.8 (carbamate *C*═O). Mass spectra, exact mass: calculated, 591.4247; found, 591.4242. Elemental analysis: calculated for $C_{33}H_{57}N_3O_6$: C, 66.97; H, 9.71; N, 7.10. Found: C, 66.89; H, 9.80; N, 7.05.

*1,3,5-Tri-N-n-heptylcarbamylphloroglucinol (**2**).* ^{1}H NMR ($CDCl_3$, 400 MHz, δ): 0.85 (t, J = 7 Hz, 9H, ω-CH_3), 1.28−1.35 (m, 24H, γ- to ω-1-CH_2), 1.47 (m, 6H, β-CH_2), 3.13 (dt, J = 6.6 and 13.4 Hz, 6H, α-CH_2), 5.37 (t, J= 6 Hz, 3H, N*H*), and 6.77 (s, 3H, benzene-*H*). ^{13}C NMR ($CDCl_3$, 100 MHz, δ): 13.9 (ω-CH_3), 22.5, 26.6, 28.8, 29.6 (γ- to ω-1-CH_2), 31.6 (β-CH_2), 41.1 (α-CH_2), 111.8 (*C*-2, *C*-4, and *C*-6 of benzene ring), 151.3 (*C*-1, *C*-3, and *C*-5 of benzene ring), and 153.6 (carbamate *C*═O). Mass spectra, exact mass: calculated, 549.3778; found, 549.3771. Elemental analysis: calculated for $C_{30}H_{51}N_3O_6$: C, 65.54; H, 9.35; N, 7.64. Found: C, 65.50; H, 9.53; N, 7.52.

*1,3,5-Tri-N-n-hexylcarbamylphloroglucinol (**3**).* ^{1}H NMR ($CDCl_3$, 400 MHz, δ): 0.86 (t, J = 7 Hz, 9H, ω-CH_3), 1.28−1.34 (m, 18H, γ- to ω-1-CH_2), 1.48 (m, 6H, β-CH_2), 3.42 (dt, J = 6.6 and 13.4 Hz, 6H, α-CH_2), 5.30 (t, J= 6 Hz, 3H, N*H*), and 6.78 (s, 3H, benzene-*H*). ^{13}C NMR ($CDCl_3$, 100 MHz, δ): 13.9 (ω-CH_3), 22.4, 26.3, 30.0 (γ- to ω-1-CH_2), 31.3 (β-CH_2), 41.2 (α-CH_2), 111.8 (*C*-2, *C*-4, and *C*-6 of benzene ring), 151.4 (*C*-1, *C*-3, and *C*-5 of benzene ring), and 153.8 (carbamate *C*═O). Mass spectra, exact mass: calculated, 507.3308; found, 507.3302. Elemental analysis: calculated for $C_{27}H_{45}N_3O_6$: C, 63.88; H,8.93; N, 8.28. Found: C, 63.79; H, 9.01; N, 8.19.

*1,3,5-Tri-N-n-butylcarbamylphloroglucinol (**4**).* ^{1}H NMR ($CDCl_3$, 400 MHz, δ): 0.90 (t, J = 7 Hz, 9H, ω-CH_3), 1.28 (sextet, J = 7 Hz, 6H, γ-CH_2), 1.45 (quintet, J = 7 Hz, 6H, β-CH_2), 3.18 (dt, J = 6.6 and 13.4 Hz, 6H, α-CH_2), 5.19 (t, J = 6 Hz, 3H, N*H*), and 6.80 (s, 3H, benzene-*H*). ^{13}C NMR ($CDCl_3$, 100 MHz, δ): 13.9 (ω-CH_3), 20.1 (γ-CH_2), 32.0 (β-CH_2), 41.1 (α-CH_2), 112.1 (*C*-2, *C*-4, and *C*-6 of benzene ring), 151.7 (*C*-1, *C*-3, and *C*-5 of benzene ring), and 154.1 (carbamate *C*═O). Mass spectra, exact mass: calculated, 423.2369; found, 424.2364. Elemental analysis: calculated for $C_{21}H_{33}N_3O_6$: C, 59.56; H,7.85; N, 9.92. Found: C, 59.51; H, 7.90; N, 9.83.

*3,5-Di-N-n-octylcarbamyloxyphenol (**5**).* ^{1}H NMR ($CDCl_3$, 400 MHz, δ): 0.86 (t, J = 7 Hz, 6H, ω-CH_3), 1.28−1.35 (m, 20H, γ- to ω-1-CH_2), 1.50 (m, 4H, β-CH_2), 3.18 (dt, J = 6.6 and 13.4 Hz, 4H, α-CH_2), 5.44 (t, J = 6.0 Hz, 2H, N*H*), 6.26−6.40 (m, 3H, benzene-*H*), and 6.42 (s, 1H, 1-OH). ^{13}C NMR ($CDCl_3$, 100 MHz, assignment from DEPT experiments, δ): 14.0 (ω-CH_3), 22.5, 26.7, 28.9, 29.1, 29.6 (γ- to ω-1-CH_2), 31.7(β-CH_2), 41.1 (α-CH_2), 106.5 (*C*-2 and *C*-4 of benzene ring), 106.8 (*C*-6 of benzene ring), 151.2 (*C*-3 and *C*-5 of benzene ring), 154.8 (*C*-1 of benzene ring) and 157.7 (carbamate *C*═O). Mass spectra, exact mass: calculated, 436.2937; found, 436.2932. Elemental analysis: calculated for $C_{24}H_{40}N_2O_5$: C, 66.03; H, 9.23; N, 6.42. Found: C, 65.96; H, 9.57; N, 6.31.

*3,5-Di-N-n-heptylcarbamyloxyphenol (**6**).* ^{1}H NMR ($CDCl_3$, 400 MHz, δ): 0.86 (t, J = 7 Hz, 6H, ω-CH_3), 1.28−1.34 (m, 16H, γ- to ω-1-CH_2), 1.50 (m, 4H, β-CH_2), 3.18 (dt, J = 6.6 and 13.4 Hz, 4H, α-CH_2), 5.44 (t, J = 6.0 Hz, 2H, N*H*), 6.22−6.24 (m, 3H, benzene-*H*), and 6.34 (s, 1H, 1-OH). ^{13}C NMR ($CDCl_3$, 100 MHz, assignment from DEPT experiments, δ): 14.0 (ω-CH_3), 22.5, 26.7, 28.9, 29.6

(γ- to ω-1-CH_2), 31.7 (β-CH_2), 41.1 (α-CH_2), 106.5 (*C*-2 and *C*-4 of benzene ring), 106.8 (*C*-6 of benzene ring), 151.2 (*C*-3 and *C*-5 of benzene ring), 154.8 (*C*-1 of benzene ring), and 157.7 (carbamate C═O). Mass spectra, exact mass: calculated, 408.2624; found, 408.2618. Elemental analysis: calculated for $C_{22}H_{36}N_2O_5$: C, 64.68; H, 8.88; N, 6.86. Found: C, 64.60; H, 9.01; N, 6.53.

*3,5-Di-N-n-hexylcarbamyloxyphenol (**7**).* ^{1}H NMR ($(CD_3)_2SO$, 400 MHz, δ): 0.86 (t, J = 7 Hz, 6H, ω-CH_3), 1.28−1.34 (m, 12H, γ- to ω-1-CH_2), 1.44 (m, 4H, β-CH_2), 3.02 (dt, J = 7 and 13 Hz, 4H, α-CH_2), 6.26−6.32 (m, 3H, benzene-*H*), and 7.68 (t, J = 5.6 Hz, 2H, N*H*), and 9.79 (s, 1H, 1-OH). ^{13}C NMR ($(CD_3)_2SO$, 100 MHz, assignment from DEPT experiments, δ): 14.0 (ω-CH_3), 22.5, 26.7, 28.9, 29.6 (γ- to ω-1-CH_2), 31.7 (β-CH_2), 41.1 (α-CH_2), 106.5 (*C*-2 and *C*-4 of benzene ring), 106.8 (*C*-6 of benzene ring), 151.2 (*C*-3 and *C*-5 of benzene ring), 154.8 (*C*-1 of benzene ring), and 157.7 (carbamate C═O). Mass spectra, exact mass: calculated, 380.2311; found, 380.2306. Elemental analysis: calculated for $C_{20}H_{32}N_2O_5$: C, 63.13; H, 8.48; N, 7.36. Found: C, 63.02; H, 8.62; N, 7.31.

*3,5-Di-N-n-butylcarbamyloxyphenol (**8**).* ^{1}H NMR ($(CD_3)_2SO$, 400 MHz, δ): 0.89 (t, J = 7 Hz, 6H, ω-CH_3), 1.29 (sextet, J = 7 Hz, 4H, γ-CH_2), 1.44 (quintet, J = 7 Hz, 4H, β-CH_2), 3.08 (dt, J = 6.6 and 13.2 Hz, 4H, α-CH_2), 6.27−6.33 (m, 3H, benzene-*H*), 7.70 (t, J = 5.6 Hz, 3H, N*H*), and 9.80 (s, 1H, 1-OH). ^{13}C NMR ($(CD_3)_2SO$, 100 MHz, δ): 13.5 (ω-CH_3), 19.4 (γ-CH_2), 31.3 (β-CH_2), 40.1 (α-CH_2), 105.4 (*C*-2 and *C*-6 of benzene ring), 105.8 (*C*-4 of benzene ring), 152.1 (*C*-1 of benzene ring), 153.9 (*C*-3 and *C*-5 of benzene ring), and 158.1 (carbamate C═O). Mass spectra, exact mass: calculated, 324.1685; found, 324.1680. Elemental analysis: calculated for $C_{16}H_{24}N_2O_5$: C, 59.24; H, 7.46; N, 8.64. Found: C, 59.11; H, 7.58; N, 8.37.

*5-N-n-Octylcarbamyloxyresorcinol (**9**).* ^{1}H NMR ($(CD_3)_2SO$, 400 MHz, δ): 0.90 (t, J = 7 Hz, 3H, ω-CH_3), 1.28−1.35 (m, 10H, γ- to ω-1-CH_2), 1.52 (m, 2H, β-CH_2), 3.21 (t, J = 6.8 Hz, 2H, α-CH_2), 4.63 (s, 1H, N*H*), 4.90 (s, 2H, 1-OH), 6.03−6.11 (m, 3H, benzene-*H*). ^{13}C NMR ($(CD_3)_2SO$, 100 MHz, assignment from DEPT experiments, δ): 14.4 (ω-CH_3), 23.6, 27.8, 30.1, 30.7, 31.8 (γ- to ω-1-CH_2), 32.9 (β-CH_2), 42.0 (α-CH_2), 100.7 (*C*-2 of benzene ring), 101.6 (*C*-4 and *C*-6 of benzene ring), 154.1 (*C*-5 of benzene ring), and 157.2 (carbamate C═O), and 159.9 (*C*-3 and *C*-5 of benzene ring). Mass spectra, exact mass: calculated, 281.1627; found, 281.1622. Elemental analysis: calculated for $C_{15}H_{23}NO_4$: C, 64.03; H, 8.24; N, 4.98. Found: C, 63.91; H, 8.37; N, 4.86.

*5-N-n-Heptylcarbamyloxyresorcinol (**10**).* ^{1}H NMR ($(CD_3)_2SO$, 400 MHz, δ): 0.89 (t, J = 7 Hz, 3H, ω-CH_3), 1.29−1.35 (m, 8H, γ- to ω-1-CH_2), 1.52 (m, 2H, β-CH_2), 3.20 (t, J = 6.8 Hz, 2H, α-CH_2), 4.63 (s, 1H, N*H*), 4.89 (s, 2H, 1-OH), 6.03−6.11 (m, 3H, benzene-*H*). ^{13}C NMR ($(CD_3)_2SO$, 100 MHz, assignment from DEPT experiments, δ): 14.4 (ω-CH_3), 23.6, 27.8, 30.7, 31.7 (γ- to ω-1-CH_2), 32.9 (β-CH_2), 42.0 (α-CH_2), 100.7 (*C*-2 of benzene ring), 101.6 (*C*-4 and *C*-6 of benzene ring), 154.1 (*C*-5 of benzene ring), and 157.2 (carbamate C═O), and 159.9 (*C*-3 and *C*-5 of benzene ring). Mass spectra, exact mass: calculated, 267.164; found, 267.158. Elemental analysis: calculated for $C_{14}H_{21}NO_4$: C, 62.90; H, 7.92; N, 5.24. Found: C, 62.78; H, 8.02; N, 5.08.

*5-N-n-Hexylcarbamyloxyresorcinol (**11**).* ^{1}H NMR ($(CD_3)_2SO$, 400 MHz, δ): 0.86 (t, J = 7 Hz, 3H, ω-CH_3), 1.29−1.35 (m, 6H, γ- to ω-1-CH_2), 1.43 (m, 2H, β-CH_2), 3.00 (dt, J = 5.6 and 6.8 Hz, 2H, α-CH_2), 5.92 (s, 2H, 4,6-benzene-*H*), 6.03 (s, 1H, 2-benzene-*H*), 7.56 (t, J = 5.2 Hz, 1H, N*H*), and 9.37 (s, 2H, 1,3-OH). ^{13}C NMR ($(CD_3)_2SO$, 100 MHz, assignment from DEPT experiments, δ): 14.7 (ω-CH_3), 22.7, 26.6, 29.9 (γ- to ω-1-CH_2), 31.6 (β-CH_2), 41.1 (α-CH_2), 99.9 (*C*-2 of benzene ring), 100.7 (*C*-4 and *C*-6 of benzene ring), 153.3(carbamate C═O), 154.8 (*C*-5 of benzene ring), and 159.2 (*C*-3 and *C*-5 of benzene ring). Mass spectra, exact mass: calculated, 253.1314; found, 253.1308. Elemental analysis: calculated for $C_{13}H_{19}NO_4$: C, 61.64; H, 7.56; N, 5.53. Found: C, 61.53; H, 7.64; N, 5.42.

*5-N-n-Butylcarbamyloxyresorcinol (**12**).* ^{1}H NMR ($(CD_3)_2SO$, 400 MHz, δ): 0.90 (t, J = 7 Hz, 3H, ω-CH_3), 1.29 (sextet, J = 7 Hz, 2H, γ-CH_2), 1.44 (quintet, J= 7 Hz, 2H, β-CH_2), 3.06 (dt, J = 6.4 and 6.8 Hz, 2H, α-CH_2), 5.93 (s, 2H, 4,6-benzene-*H*), 6.04 (s, 1H, 2-benzene-*H*), 7.57 (t, J = 5.2 Hz, 1H, N*H*), and 9.36 (s, 2H, 1,3-OH).

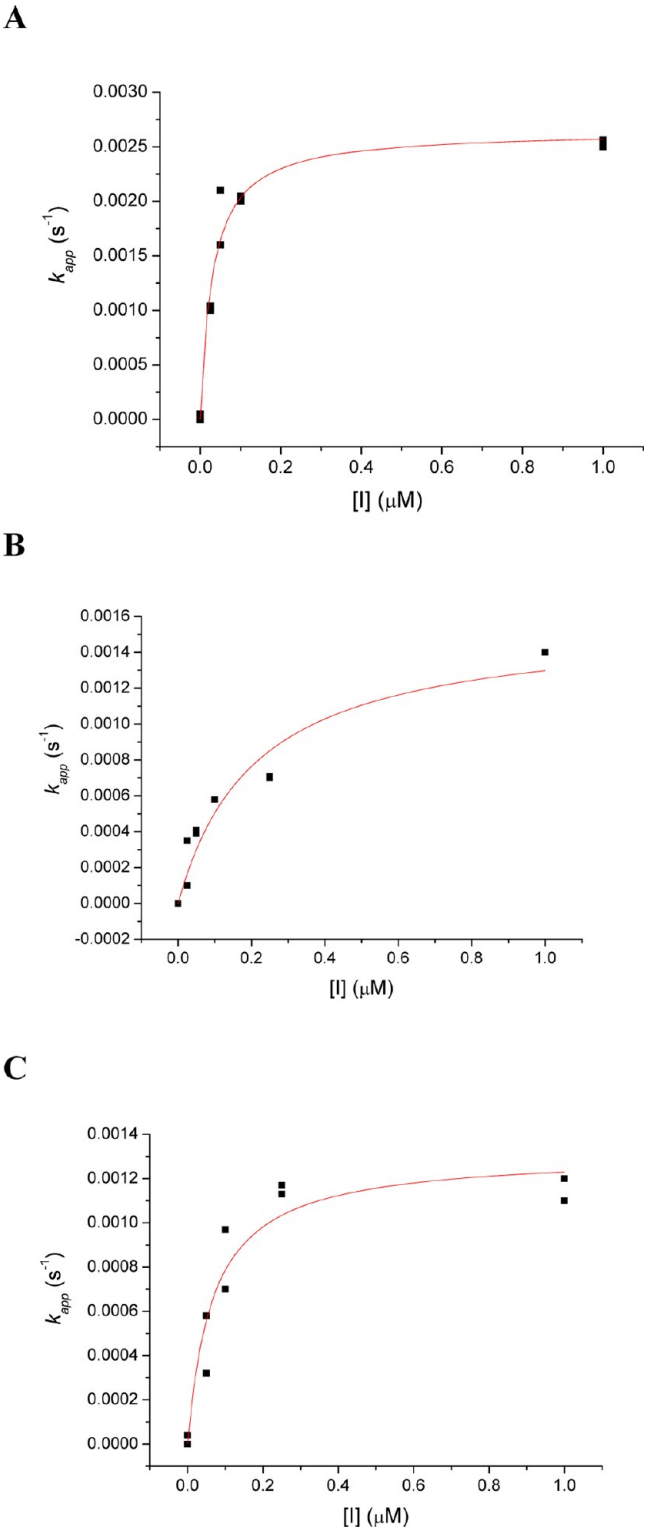

Figure 4. Nonlinear least-squares curve fittings of k_{app} vs inhibitor concentration ([I]) plots against eq 1 for the pseudo substrate inhibition of AChE by 1,3,5-tri-*N*-*n*-octylcarbamylphloroglucinol (**1**) (A), 3,5-di-*N*-*n*-hexylcarbamyloxy-phenol (**7**) (B), and 5-*N*-*n*-heptylcarbamyloxyresorcinol (**10**) (C). For A, k_2 = 0.0027 ± 0.0001 s^{-1} and K_i = 15 ± 3 nM (R^2 = 0.96458). For B, k_2 = 0.0016 ± 0.0002 s^{-1} and K_i = 110 ± 40 nM (R^2 = 0.91316). For C, k_2 = 0.0018 ± 0.0002 s^{-1} and K_i = 60 ± 20 nM (R^2 = 0.92569).

^{13}C NMR ($(CD_3)_2SO$, 100 MHz, assignment from DEPT experiments, δ): 13.551 (ω-CH_3), 19.4 (γ-CH_2), 31.3 (β-CH_2), 40.3 (α-CH_2), 105.0 (*C*-2 of

dx.doi.org/10.1021/tx300119a | *Chem. Res. Toxicol.* 2012, 25, 1462−1471

Table 1. Pseudo Substrate Inhibition Constants of AChE by Inhibitors 1−12

inhibitors	k_2 (10^{-3} s^{-1})	K_i (nM)	k_i (10^3 M^{-1} s^{-1})	k_3 (10^{-4} s^{-1})
1	2.7 ± 0.1[a]	15 ± 3	180 ± 40	1.2 ± 0.2
2	2.2 ± 0.1	34 ± 7	60 ± 10	1.8 ± 0.2
3	2.5 ± 0.2	81 ± 15	31 ± 6	2.7 ± 0.3
4	2.3 ± 0.5	30 ± 10	80 ± 30	3.5 ± 0.3
5	2.6 ± 0.1	100 ± 30	26 ± 9	1.1 ± 0.1
6	2.7 ± 0.1	110 ± 40	25 ± 9	1.8 ± 0.2
7	1.6 ± 0.2	110 ± 40	15 ± 5	2.6 ± 0.3
8	2.1 ± 0.2	100 ± 20	21 ± 5	3.4 ± 0.3
9	1.54 ± 0.08	31 ± 6	50 ± 10	1.1 ± 0.1
10	1.3 ± 0.1	34 ± 10	40 ± 10	1.7 ± 0.2
11	1.8 ± 0.2	60 ± 20	30 ± 10	2.8 ± 0.3
12	1.3 ± 0.1	80 ± 20	16 ± 4	3.3 ± 0.3
donepezil		35 ± 4[b]		

[a]The k_i values were calculated from k_2/K_i and uncertainty in k_i values = [(uncertainty of k_2)^2 + (uncertainty of K_i)^2]$^{1/2}$. [b]K_i = 21 ± 3 nM from Piazzi et al.[39]

benzene ring), 106.0 (*C*-4 and *C*-6 of benzene ring), 155.6 (carbamate *C*═O), 156.0 (*C*-5 of benzene ring), and 162.0 (*C*-3 and *C*-5 of benzene ring). Mass spectra, exact mass: calculated, 225.1001; found, 225.0095. Elemental analysis: calculated for $C_{11}H_{15}NO_4$: C, 58.66; H, 6.71; N, 6.22. Found: C,58.58; H, 6.90; N, 6.13.

Instrumental Methods. ^{1}H and ^{13}C NMR spectra were recorded at 400 and 100 MHz, respectively, on a Varian-Gemini 400 spectrometer with an internal reference tetramethylsilane at 25 °C. Mass spectra were recorded at 71 eV in a mass spectrometer (Joel JMS-SX/SX 102A). Elemental analyses were preformed on a Heraeus instrument. All steady state kinetic data were obtained from a UV−visible spectrometer (Agilent 8453) with a cell holder circulated with a water bath.

Data Reduction. Origin (version 6.0) was used for the linear and nonlinear least-squares curve fittings.

AChE Inhibition. The inhibition reactions of AChE were determined by the Ellman assay.[32] The AChE-catalyzed hydrolysis of substrate acetylthiocholine (0.1 mM) in the presence of 5,5′-dithio-bis-2-nitrobenzoate (0.1 mM) and inhibitors **1**−**12** were followed continuously at 410 nm on a UV−visible spectrometer at 25 °C, pH 7.1. The temperature was maintained at 25.0 °C by a refrigerated circulating water bath. All reactions were preformed in sodium phosphate buffer (1 mL, 0.1 M, pH 7.1) containing NaCl (0.1 M), CH_3CN (2% by volume), detergent triton-X 100 (TX) (0.5% by weight), substrate acetylthiocholine (K_m = 0.10 ± 0.01 mM), and a varying concentration of the inhibitors. Requisite volumes of stock solution of substrate acetylthiocholine and the inhibitor in acetonitrile were injected into reaction buffer via a pipet. The reaction was followed until 85% of substrate consumption was completed. The K_i and k_2 values were obtained from the nonlinear least-squares of curve fittings of the k_{app} values versus inhibition concentration ([I]) plot against eq 1[5] (Figure 4 and Table 1). The carbamylation stage is rapid as compared to subsequent decarbamylation ($k_2 \gg k_3$); thus, the two stages are easily resolved kinetically. Values of decarbamylation constants (k_3 values) were determined from the first order rate constants for the percent activity versus time plots (Figure 5).[33] The percent activity was defined as V_i/V_0, where V_i is the initial rate for an inhibitor incubated with AChE for a period of time (T) and V_0 is the initial rate of AChE at time T without an inhibitor. Duplicate sets of data were collected for each inhibitor concentration.

AChE Catalyzed the Hydrolysis of Tridentate 1. Powder of AChE from *Electrophorus electricus* (500 units) was added to a 1 mL of phosphate buffer solution (0.1 M, pH 7.1) of **1** (100 mM) at 37 °C. The progress of the reaction was monitored by TLC (the R_f values of tridentate **1**, didentate **5**, monodentate **9**, and phloroglucinol were 0.65, 0.25, 0.1, and 0, respectively, developed in hexane−ethyl acetate (5/1, v/v)). After 30 min, [tridentate **1**]:[didentate **5**]:[monodentate **9**]:[phloroglucinol] is about 1:6:2:1. After 5 h, the ratio became 1:2:4:3. Therefore, these results suggested that AChE catalyzed the hydrolyses of tridentate **1** to didentate **5**, didentate **5** to monodentate **9**, and monodentate **9** to phloroglucinol (Figure 3).

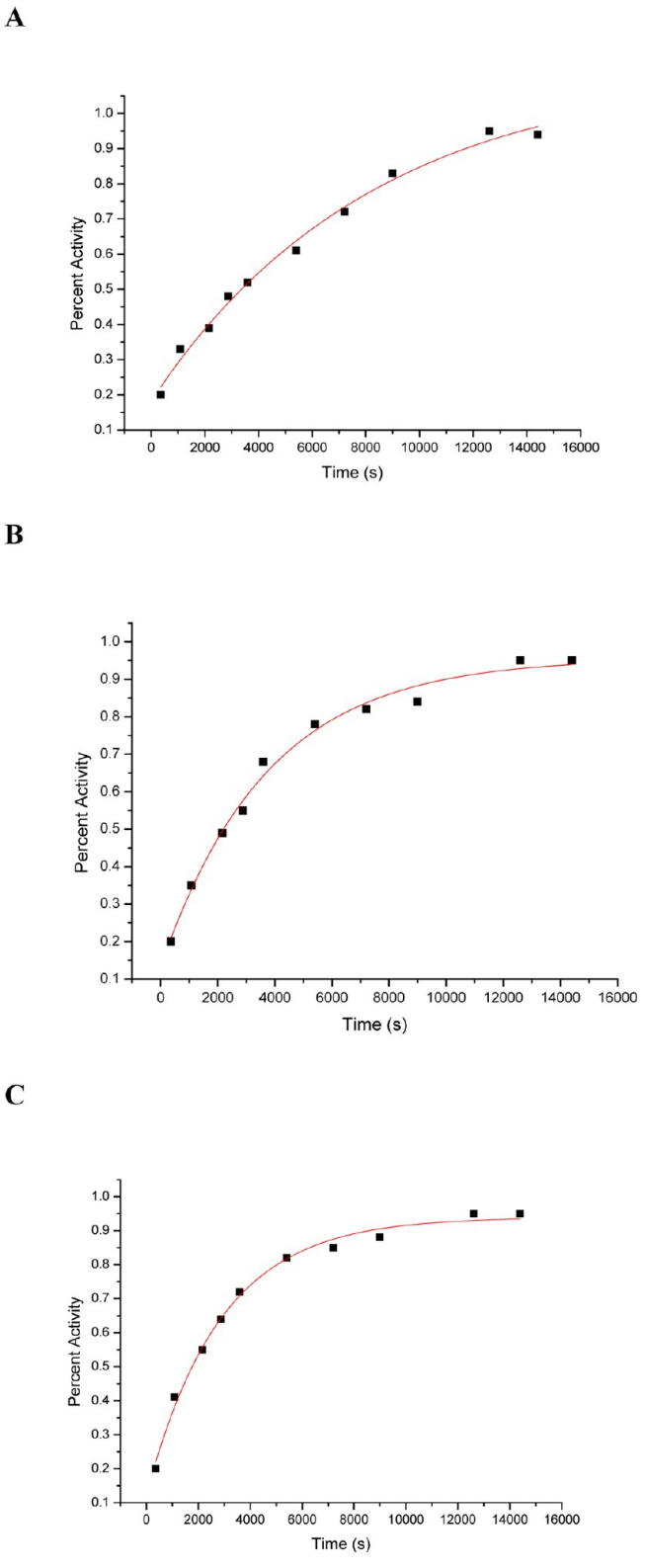

Figure 5. Decarbamylation constant (k_3). The first order rate process for the time course of percent activity for the pseudo substrate inhibition[33] of PSL by 1,3,5-tri-*N*-*n*-octylcarbamylphloroglucinol (**1**) (A), 1,3,5-tri-*N*-*n*-hexylcarbamyl- phloroglucinol (**3**) (B), and 1,3,5-tri-*N*-*n*-butylcarbamylphloroglucinol (**4**) (C). For A, k_3 = (1.2 ± 0.2) × 10^{-4} s^{-1} (R^2 = 0.99037). For B, k_3 = (2.7 ± 0.3) × 10^{-4} s^{-1} (R^2 = 0.98855). For C, k_3 = (3.5 ± 0.3) × 10^{-4} s^{-1} (R^2 = 0.99232).

dx.doi.org/10.1021/tx300119a | *Chem. Res. Toxicol.* 2012, 25, 1462−1471

Molecular Modeling of Inhibitors and Automated Docking Inhibitors into AChE. Molecular structures of (1,3,5)-(*cis,trans,trans*)- and (*trans,trans,trans*)-tricarbamate conformation of inhibitor **1** were depicted from the molecular structures after MM-2 energy minimization (minimum root-mean-square gradient was set to be 0.01) by CS Chem 3D (version 6.0). Out of all of the entries for AChE from RCSB protein data bank, mouse AChE (2HA3)[4] and recombinant human AChE (3lii)[45] were taken for docking analysis. Protein-inhibitor docking studies were performed to evaluate the algorithm and scoring function efficiency between a standalone AutoDock 4.2[34−37] and experimental activities. Automated docking was used to locate the appropriate binding orientations and conformations of various inhibitors in the enzyme binding pocket. All water molecules were removed from the original Protein Data Bank file. Polar hydrogen atoms were added, and Kollman charge, atomic solvation parameters, and fragmental volumes were assigned to the protein using AutoDock Tools (ADT). For docking calculations, Gasteiger partial charges were assigned to the tested derivatives, and nonpolar hydrogen atoms were merged. The torsions of C−O and carbamate CN partial double bonds were allowed (Figure 8) or restricted (Figure 9) to rotate during docking. The program AutoGrid used to generate the grid maps. Each grid was centered at the crystal structure of the corresponding enzyme. The grid dimensions were 40 × 40 × 40 Å^3 with points separated by 0.375 Å. For all inhibitors, random starting positions, random orientations, and torsions were used. The translation, quaternion, and torsion steps were taken from default values in AutoDock. The Lamarckian genetic algorithm and the pseudo-Solids and Wets methods were applied for minimization using default parameters. The standard docking protocol for rigid and flexible inhibitor docking consisted of 50 independent runs per inhibitor, using an initial population of 150 randomly placed individuals, with 2.5 × 10^6 energy evaluations, a maximum number of 27000 iterations, a mutation rate of 0.02, a crossover rate of 0.80, and an elitism value of 1. The probability of performing a local search on an individual in the population was 0.06, using a maximum of 300 iterations per local search. After docking, the 10 solutions were clustered into groups with rms deviations lower than 1.0 Å. The clusters were ranked by the lowest energy representative of each cluster. The interactive visualization and analysis of molecular structures and hydrogen bonds between protein and inhibitor were preformed by UCSF Chimera.[38]

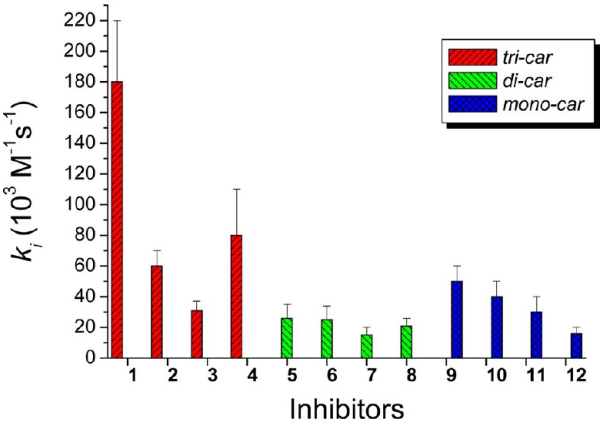

Figure 6. Comparisons of the k_i values of pseudo substrate inhibitions of AChE by inhibitors **1**−**12**.

RESULTS

1,3,5-Tri-*N*-*n*-alkylcarbamylphloroglucinols (**1**−**4**), 3,5-di-*N*-*n*-alkylcarbamyloxy-phenols (**5**−**8**), and 5-*N*-*n*-alkylcarbamyloxyresorcinols (**9**−**12**) (Figure 2) were synthesized from one pot reaction of phloroglucinol with 2 equiv of the corresponding *n*-alkylisocyanate and 2 equiv of triethylamine in tetrahydrofuran at 25 °C for 5 h. Three products were easily separated by liquid chromatography. Under this optimal condition, the product ratio for 1,3,5-tri-*N*-*n*-alkylcarbamylphloroglucinols (**1**−**4**):3,5-di-*N*-*n*-alkylcarbamyloxyphenols (**5**−**8**):5-*N*-*n*-alkylcarbamyloxyresorcinols (**9**−**12**) was about 2:1:1.5. When 3 equiv

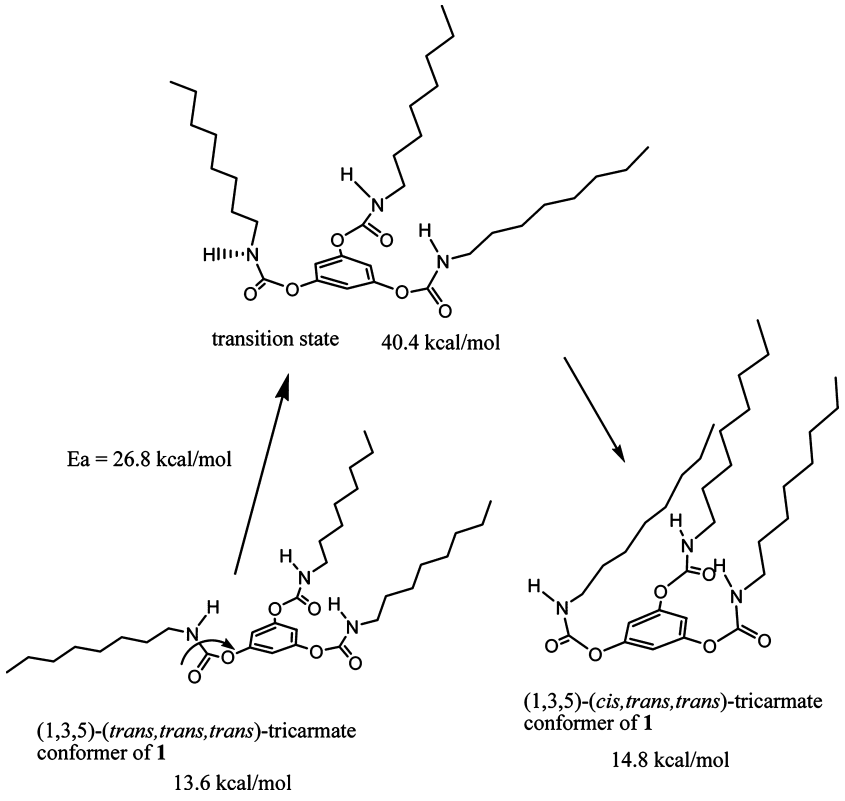

Figure 7. Conformational changes between (1,3,5)-(*trans,trans,trans*)- and (1,3,5)-(*cis,trans,trans*)-tricarbamate rotamers of inhibitor **1**.

dx.doi.org/10.1021/tx300119a | *Chem. Res. Toxicol.* 2012, 25, 1462−1471

of *n*-alkylisocyanate and 3 equiv of triethylamine were used, the reactions only yielded 1,3,5-tri-*N*-*n*-alkylcarbamylphloroglucinols (**1**−**4**). When 1 equiv of *n*-alkylisocyanate and 1 equiv of triethylamine were used, the reaction yield is too low.

Carbamate inhibitors **1**−**12** were all characterized as the pseudo substrate inhibitors of AChE (Figures 1, 4, and 5 and Table 1). It is assumed that AChE catalyzes the hydrolysis of one *n*-alkylcarbamyl group of inhibitors **1**−**12** (Figure 3). In other words, inhibitors **1**−**12** may react with the enzyme through the nucleophilic attack of the catalytic serine of the enzyme to one carbamyl carbon of inhibitors **1**−**12**.

For AChE inhibition, the inhibitory potencies are as follows: tridentate inhibitors 1,3,5-tri-*N*-*n*-alkylcarbamylphloroglucinols (**1**−**4**) > monodentate inhibitors 5-*N*-*n*-alkylcarbamyloxyresorcinols (**9**−**12**) > bidentate inhibitors 3,5-di-*N*-*n*-alkylcarbamyloxyphenols (**5**−**8**) (Figure 6 and Table 1). Tridentate inhibitors 1,3,5-tri-*N*-*n*-alkylcarbamylphloroglucinols (**1**−**4**) were the most potent inhibitors (Figure 6). Comparison of different alkyl substituents of inhibitors **1**−**4** indicates that *n*-octylcarbamyl inhibitor **1** is the most potent inhibitors (Figure 6 and Table 1). The K_i value of inhibitor **1** is about the same with that of donepezil.[39]

The (1,3,5)-(*trans*,*trans*,*trans*)-tricarbamate rotamer of **1** can better bind to AChE when the configuration is changed to (1,3,5)-(*cis*,*trans*,*trans*) rotamer. Molecular docking of the most stable (1,3,5)-(*trans*,*trans*,*trans*)-tricarbamate rotamer of inhibitor **1** (Figure 7) into the X-ray crystal structure of mouse AChE results that (1,3,5)-(*cis*,*trans*,*trans*)-tricarbamate rotamer is the most optimal configuration for the enzyme binding (Figure 8). Separate docking of (1,3,5)-(*trans*,*trans*,*trans*)- and (1,3,5)-(*cis*,*trans*,*trans*)-tricarbamate rotamers (Figure 7) into the enzyme by restricted rotation of the CN partial double

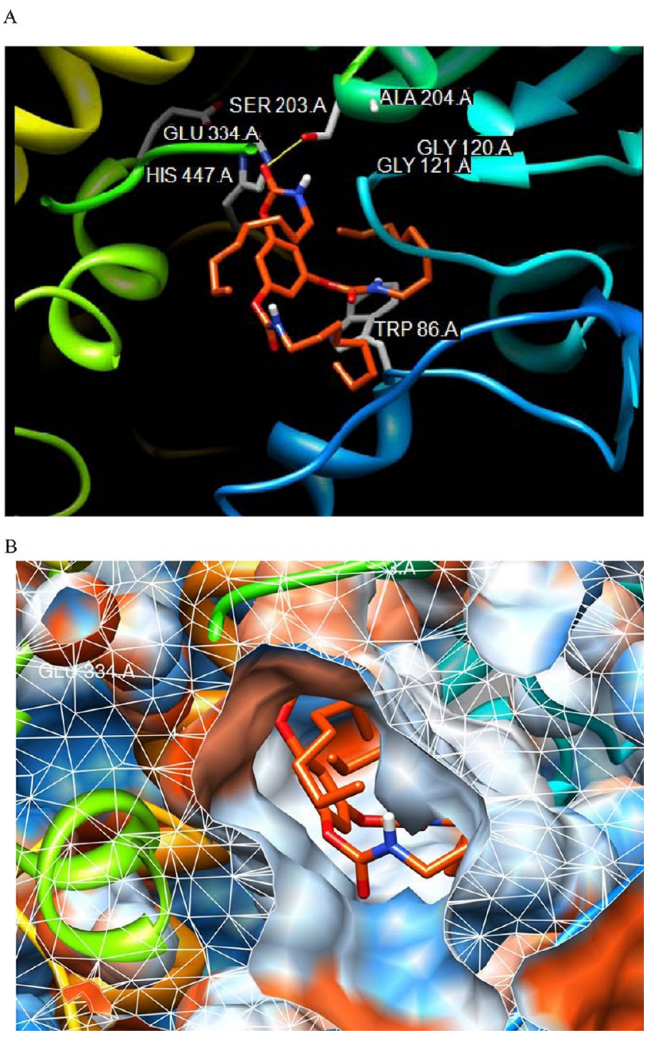

Figure 8. Molecular docking of tridentate inhibitor **1**, with the mode of free rotation around the carbamyl CN partial double bond, into the active sites of X-ray crystal structure of mouse AChE (2HA3):[4] (A) the active site view and (B) the view from the entrance (mouth) of the enzyme. The configuration of the inhibitor after docked is the (1,3,5)-(*cis*,*trans*,*trans*)-tricarbamate rotamer. The carbamyl carbonyl carbon atom of the inhibitor is close to S203 of the catalytic triad, and the carbamyl ester oxygen atom of the inhibitor is closed to H447 of the catalytic triad. Two octylcarbamyl groups of the inhibitor shield W86 of the enzyme.

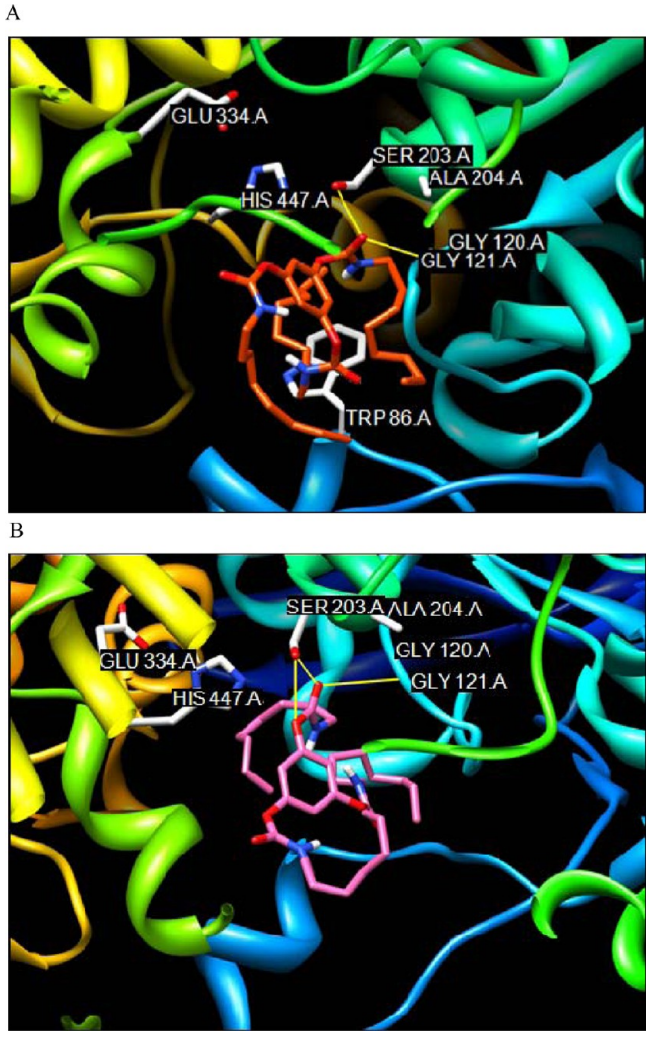

Figure 9. Molecular docking of (1,3,5)-(*trans*,*trans*,*trans*)-tricarbamate rotamer of inhibitor **1**, with restricted rotations of the carbamyl CN partial double bonds, into the active sites of X-ray crystal structure of mouse AChE (2HA3)[4] results in two unlikely binding modes. (A) The carbamyl ester oxygen atom of the inhibitor is too far away from H447 of the catalytic triad. Therefore, this rotamer is not a pseudo substrate inhibitor of the enzyme. (B) An octylcarbamy group of this rotamer blocks the hydrogen bond formation between the carbamyl ester oxygen atom of the inhibitor and the H447 of the catalytic triad. Therefore, this rotamer can not react with the enzyme.

dx.doi.org/10.1021/tx300119a | *Chem. Res. Toxicol.* 2012, 25, 1462−1471

bonds of inhibitors suggests that the former rotamer is less likely to bind into the enzyme (Figure 9), but the latter rotamer binds well into the enzyme (Figure 8).

DISCUSSION

Inhibitory Potencies for Mono-, Bi-, and Tridentate-*n*-alkylcarbamyl-phloroglucinols. For AChE inhibition, the inhibitory potencies are as follows: tridentate inhibitors 1,3,5-tri-*N*-*n*-alkylcarbamylphloroglucinols (**1**−**4**) > monodentate inhibitors 5-*N*-*n*-alkylcarbamyloxyresorcinols (**9**−**12**) > bidentate inhibitors 3,5-di-*N*-*n*-alkylcarbamyloxyphenols (**5**−**8**) (Table 1 and Figure 6). For tridentate inhibitors **1**−**4**, one carbamyl group extends to the entrance, and the other two carbamyl groups bind to W86 of AS of the enzyme (Figure 8). For bidentate inhibitors 3,5-di-*N*-alkylcarbamyloxyphenols (**5**−**8**), one carbamyl group extends to the entrance, and the other one may bind to W86 of AS of the enzyme. In the meanwhile, the hydroxyl groups of inhibitors **5**−**8** are also close to W86. This encounter (hydrophilic group and tryptophan π orbital) may weaken the binding between the inhibitor and the W86 of AS of the enzyme and may cause the reason why inhibitors **5**−**8** become the worst inhibitors of AChE among inhibitors **1**−**12**.

Inhibitory Potencies for Varied the Chain Lengths of *n*-Alkylcarbamyl Moieties of Inhibitors 1−12. Comparison of different alkyl substituents of inhibitors **1**−**4** indicates that *n*-octylcarbamyl inhibitor **1** is the most potent inhibitor (Figure 6 and Table 1). One of three *n*-octylcarbamyl moieties of inhibitor **1** may extend itself to the entrance or PAS of the enzyme (Figure 8). Therefore, the longer the carbamy moieties of the inhibitors carry, the more potent of these inhibitors are.

The k_2 values of AChE inhibition by tridentate inhibitors **1**−**12** retain constant when varied with the carbamyl chain length (Table 1). The optimal substrate chain for acetyl group binding site (ABS) for AChE is the acetyl group as in ACh. Therefore, most parts of the alkylcarbamyl moieties of monodentate inhibitors **1**−**12** in the AChE-inhibitor tetrahedral intermediate may not bind inside the acetyl binding site (ABS) but outside ABS. The alkylcarbamyl moieties of inhibitors **1**−**12** repulse with the leaving group parts of the inhibitors in these tetrahedral intermediates. These repulsions make all inhibitors **1**−**12** have similar k_2 values ($1.3-2.7 \times 10^{-3}$ s^{-1}). For log k_i and pK_i values of inhibitors **1**−**12**, only those of monodentate inhibitors exist in linear relationships with the alkyl group chain length of the alkyl chain of the inhibitors (n) or the hydrophobicity constant (π), which is defined as $n/2$ (Figure 10).[40,41] Thus, the *n*-alkylcarbamyl groups of monodentate inhibitors **9**−**12** may bind to the enzyme through a common mechanism (or at the same binding sites). The longer carbamyl groups of monodentate inhibitors **9**−**12** may bind better to the enzyme.[9,10] On the other hand, tridentate inhibitors **1**−**4** and bidentate inhibitors **5**−**8** may bind to the enzyme with different mechanisms or at different binding sites.

Long-Lived Tridentate Inhibitors. Tridentate inhibitors **1**−**4** act as the pseudo substrate inhibitors of AChE (Figure 1 and Table 1).[5−15] The pseudo substrate inhibition reactions of tridentate inhibitors **1**−**4** yield bidentate inhibitors **5**−**8** that are also characterized as the pseudo substrate inhibitors of the enzyme (Figure 3 and Table 1). The pseudo substrate inhibition reactions of bidentate inhibitors **5**−**8** yield monodentate inhibitors **9**−**12** that are also the pseudo substrate inhibitors of the enzyme (Figure 3 and Table 1). Accordingly, tridentate inhibitors **1**−**4** may act as long-lived inhibitors of AChE.

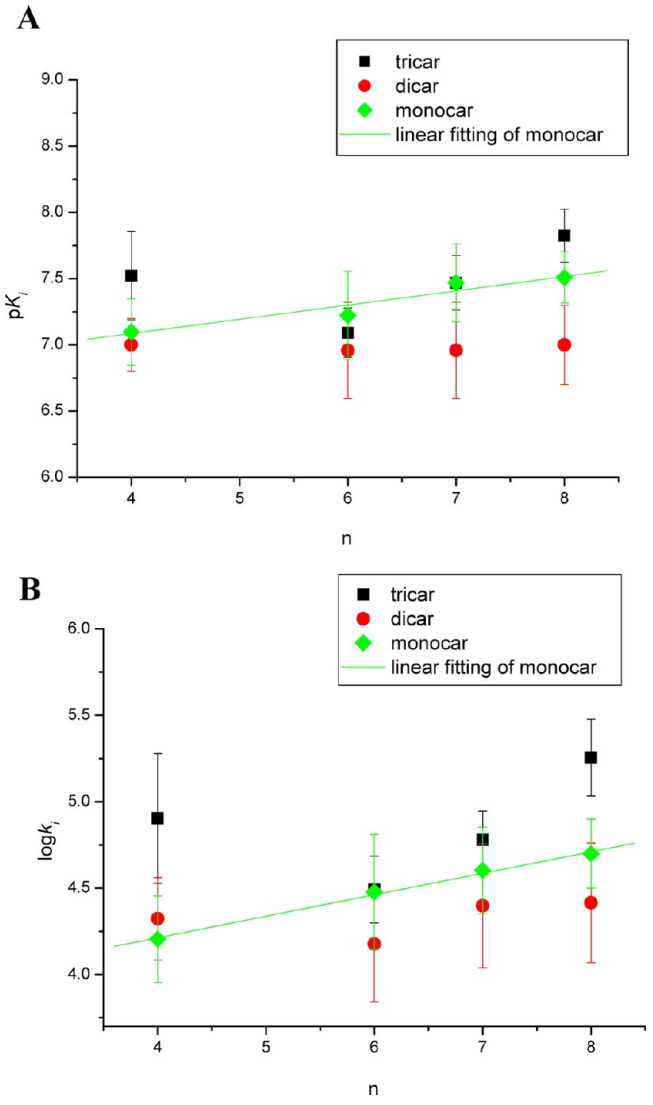

Figure 10. pK_i (A) and log k_i values vs carbamyl carbon numbers (n) of inhibitors **1**−**12** for the pseudo substrate inhibition of AChE. (A) For monodentate inhibitors **9**−**12**, a linear correlation between pK_i and n is observed [pK_i = 6.7 ± 0.1 + (0.10 ± 0.02)n; R = 0.97439]. (B) For monodentate inhibitors **9**−**12**, a linear correlation between log k_i and n is observed [log k_i = 3.71 ± 0.04 + (0.124 ± 0.006)n; R = 0.99786].

Docking of Inhibitor 1 into the X-ray Crystal Structure of AChE. Conformational analysis of inhibitor **1** by MM-2 suggests that the most two stable rotamers are (1,3,5)-(*trans*,*trans*,*trans*)- and (1,3,5)-(*cis*,*trans*,*trans*)-tricarbamate forms (Figure 7). The energy barrier from the all-*trans*- to (*cis*,*trans*,*trans*)-**1** is calculated to be 38 kJ/mol by variations of both bond angles and bond lengths from semiempirical method (unpublished result). This activation energy is relative; therefore, these two rotamers can easily convert to each other even at −10 °C.[42]

The result of molecular docking suggests that AChE selectively binds to the (1,3,5)-(*cis*,*trans*,*trans*)-tricarbamate form among many conformations of inhibitor **1** (Figure 7). In this docking, the *cis* carbamy group of the (*cis*,*trans*,*trans*)-rotamer of **1** does not bind into the ABS but reaches out itself into the entrance as the X-ray crystal structure of the long chain carbamylated AChE.[43] Both *trans* carbamyl moieties of

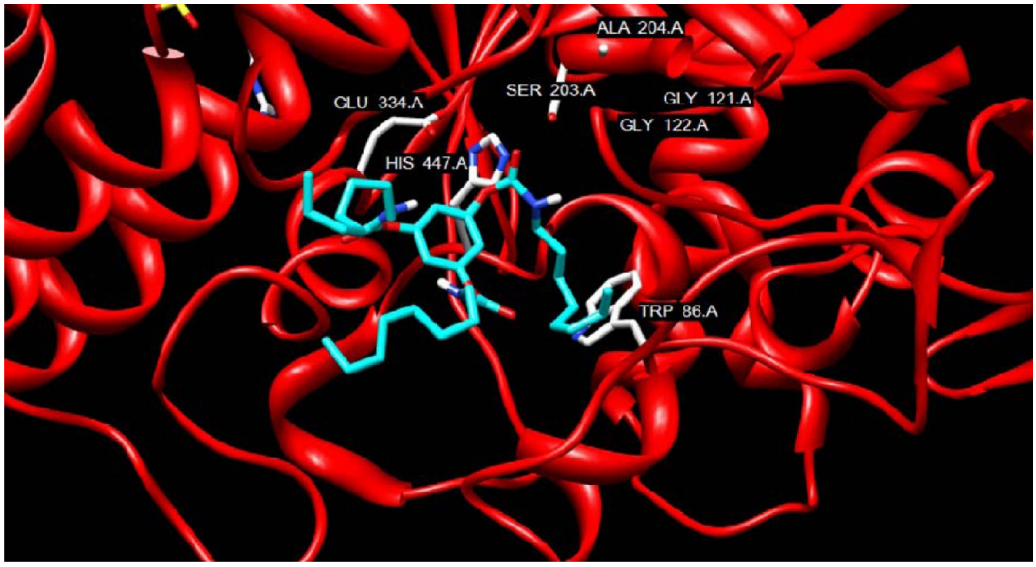

Figure 11. Molecular docking of (1,3,5)-(*trans*,*trans*,*trans*)-tricarbamate rotamer of inhibitor **1** into the active sites of X-ray crystal structure of recombinant human AChE (3lii).[45] The carbamyl carbonyl carbon atom of the inhibitor is close to S203 of the catalytic triad, and the carbamyl ester oxygen atom of the inhibitor is closed to H447 of the catalytic triad. One octylcarbamyl group of the inhibitor binds to W86 of the enzyme.

(*cis*,*trans*,*trans*)-rotamer of **1** bind very well into W86 of the AS. From another side view, this form completely blocks the entrance of the enzyme (Figure 8B).

Molecular docking of (1,3,5)-(*trans*,*trans*,*trans*)-tricarbamate rotamer of **1** into AChE results in two unlikely binding modes (Figure 9). In Figure 9A, the carbamyl ester oxygen of the all-*trans* rotamer is too far away from H447 of the catalytic triad. Therefore, the all-*trans* rotamer unlikely acts as the pseudo substrate inhibitor of the enzyme. In Figure 9B, the alkyl chain of the carbamy group of the all-*trans* rotamer blocks the hydrogen bond formation between the carbamyl ester oxygen of the inhibitor and the H447 of the catalytic triad. Therefore, the all-*trans* rotamer can not also react with the enzyme. Thus, it can be concluded that (1,3,5)-(*trans*,*trans*,*trans*)- tricarbamate rotamer of **1** is not the right configuration for the AChE binding.

Recently, X-ray crystal structures of human AChE complexed with fasciculin II[44] and recombinant human AChE[45] have been reported. Molecular docking of (1,3,5)-(*cis*,*trans*,*trans*)-tricarbamate rotamer of inhibitor **1** into the X-ray crystal structure of recombinant human AChE (3lii) indicates that a peptide sequence of the enzyme and the inhibitor, together, block the active site gorge (Figure 11).

AUTHOR INFORMATION

Corresponding Author

*E-mail: gilin@dragon.nchu.edu.tw.

Funding

This work was supported by National Science Council of Taiwan (NSC 100-2113-M-005-003).

Notes

The authors declare no competing financial interest.

ABBREVIATIONS

ABS, acetyl group binding site; ACh, acetylcholine; AChE, acetylcholinesterase; AS, anionic substrate binding site; BChE, butyrylcholinesterase; DTNB, 5,5′-dithiobis-(2-nitrobenzoic acid); ES, esteratic site or catalytic triad; OAH, oxyanion hole; PAS, peripheral anionic substrate binding site

REFERENCES

(1) Quinn, D. M. (1987) Acetylcholinesterase: Enzyme structure, reaction dynamics, and virtual transition states. *Chem. Rev. 87*, 955−979.

(2) Sussman, J. L., Harel, M., Frolow, F., Oefner, C., Goldman, A., Toker, L., and Silman, I. (1991) Atomic structure of acetylcholinesterase from *Torpedo californica*: A prototypic acetylcholine-binding protein. *Science 253*, 872−879.

(3) Bar-On, P., Millard, C. B., Harel, M., Dvir, H., Enz, A., Sussman, J. L., and Silman, I. (2002) Kinetic and structural studies on the interaction of cholinesterase with anti-Alzheimer drug rivastigmine. *Biochemistry 41*, 3555−3564.

(4) Bourne, Y., Radić, Z., Sulzenbacher, G., Kim, E., Taylor, P., and Marchot, P. (2006) Substrate and product trafficking through the active center gorge of acetylcholinesterase analyzed by crystallography and equilibrium binding. *J. Biol. Chem. 281*, 29256−29267.

(5) Hosie, L., Sutton, L. D., and Quinn, D. M. (1987) *p*-Nitrophenyl and cholesteryl-*N*-alkyl carbamates as inhibitors of cholesterol esterase. *J. Biol. Chem. 262*, 260−264.

(6) Lin, G., and Lai, C.-Y. (1995) Hammett analysis of the inhibition of pancreatic cholesterol esterase by substituted phenyl-N-butylcarbamate. *Tetrahedron Lett. 36*, 6117−6120.

(7) Lin, G., Chen, G.-H., Yeh, S.-C., and Lu, C.-P. (2005) Probing the peripheral anionic site of acetylcholinesterase with quantitative structure activity relationships for the inhibitions by biphenyl-4-acyoxylate-4′-*N*-butylcarbamates. *J. Biochem. Mol. Toxicol. 19*, 234−243.

(8) Lin, M.-C., Hwang, M.-T., Chang, H.-G., Lin, C.-S., and Lin, G. (2007) Benzene-1,2-, 1,3-, and 1,4-di-N-substituted carbamates as conformationally constrained inhibitors of acetylcholinesterase. *J. Biochem. Mol. Toxicol. 21*, 348−353.

(9) Lin, G., Tseng, H.-C., Chio, A.-C., Tseng, T.-M., and Tsai, B.-Y. (2005) A rate determining step change in the pre-steady state of acetylcholinesterase inhibitions by 1,n-alkane-di-*N*-butycarbamates. *Bioorg. Med. Chem. Lett. 15*, 951−955.

(10) Lin, G., Shieh, C.-T., Ho, H.-C., Chouhwang, J.-Y., Lin, W.-Y., and Lu, C.-P. (1999) Structure-reactivity relationships for the inhibition mechanism at the second alkyl-chain-binding site of cholesterol esterase and lipase. *Biochemistry 38*, 9971−9981.

(11) Pietsch, M., Christian, L., Inhester, T., Petzold, S., and Gütschow, M. (2009) Kinetics of inhibition of acetylcholinesterase in the presence of acetinotile. *FEBS J. 276*, 2292−2307.

(12) Luo, W., Yu, Q.-S., Kulkami, S. S., Parrish, D. A., Holloway, H. W., Tweedie, D., Shafferman, A., Lahiri, D. K., Brossi, A., and Greig, N. H. (2006) Inhibition of human acetyl- and butyrylcholinesterase by novel carbamates of (-)- and (+)-tetrahydrofurobenzofuran and methanobenzodioxepine. *J. Med. Chem. 49*, 2174−2185.
(13) Darvesh, S., Darvesh, K. V., McDonald, R. S., Mataija, R., Walsh, R., Mothana, S., Lockridge, O., and Martin, E. (2008) Carbamates with differential mechanism of inhibition toward acetylcholinesterase and butyrylcholinesterase. *J. Med. Chem. 51*, 4200−4212.
(14) Pietsch, M., and Gütschow, M. (2002) Alternate substrate inhibition of cholesterol esterase by thieno[2,3-d][1,3]oxazin-4-ones. *J. Biol. Chem. 277*, 24006−24013.
(15) Pietsch, M., and Gütschow, M. (2005) Synthesis of tricyclic 1,3-oxazin-4-ones and kinetic analysis of cholesterol esterase and acetylcholinesterase inhibition. *J. Med. Chem. 48*, 8270−8288.
(16) Pang, Y.-P., Quiram, P., Jelacic, T., Hong, F., and Brimijoin, S. (1996) Highly potent, selective, and low cost bis-tetrahydroaminacrine inhibitors of acetylcholinesterase. *J. Biol. Chem. 271*, 23646−23649.
(17) Haviv, H., Wong, D. M., Greenblatt, H. M., Carlier, P. R., Pang, Y.-P., Silman, I., and Sussman, J. L. (2005) Crystal packing mediates enantioselective ligand recognition at the peripheral site of acetylcholinesterase. *J. Am. Chem. Soc. 127*, 11029−11036.
(18) Rydberg, E. H., Brumshein, B., Greenblatt, H. M., Wong, D. M., Shaya, D., Williams, L. D., Carlier, P. R., Pang, Y.-P., Silman, I., and Sussman, J. L. (2006) Complexes of alkylene-linked tacrine dimers with *Topedo californica* acetylcholinesterase: Binding of bis(5)-tacrine produce a dramatic rearrangement in the active-site gorge. *J. Med. Chem. 49*, 5491−5500.
(19) Colletier, J. P., Sanson, B., Nachon, F., Gabelleri, E., Fattorusso, C., Campiani, G., and Weik, M. (2006) Conformational flexibility in the peripheral site of *Topedo californica* acetylcholinesterase revealed by the complex structure with a bifunctional inhibitor. *J. Am. Chem. Soc. 128*, 4526−4527.
(20) Bolognesi, M. L., Cavalli, A., Valgimigli, L., Bartolini, M., Rosini, M., Andrisano, V., Recanatini, M., and Melchiorre, C. (2007) Multi-target-directed drug design strategy from a dual binding site acetylcholinesterase inhibitor to a trifunctional compound against Alzheimer's disease. *J. Med. Chem. 50*, 6446−6449.
(21) Johnson, J. L., Cusack, B., Hughes, T. F., McCullough, E. H., Fauq, A., Romanovskis, P., Spatola, A. F., and Rosenberry, T. L. (2003) Inhibitors tethered near the acetylcholinesterase active site serve as molecular rulers of the peripheral and acylation sites. *J. Biol. Chem. 278*, 38948−38955.
(22) He, X.-C., Feng, S., Wang, Z.-F., Shi, Y., Zheng, S., Xia, Y., Jiang, H., Tang, X.-C., and Bai, D. (2007) Study on dual-site inhibitors of acetylcholinesterase: Highly potent derivatives of bis- and bifunctional huperzine B. *Bioorg. Med. Chem. 15*, 1394−1408.
(23) Feng, S., Wang, Z., He, X., Zheng, S., Xia, Y., Jiang, H., Tang, X., and Bai, D. (2005) Bis-huperzine B: Highly potent and selective acetylcholinesterase inhibitors. *J. Med. Chem. 48*, 655−657.
(24) Xie, Q., Wang, H., Xia, Z., Lu, M., Zhang, W., Wang, X., Fu, W., Tang, Y., Sheng, W., Li, W., Zhou, W., Zhu, X., Qiu, Z., and Chen, H. (2008) Bis-(-)-nor-meptazinols as novel nanomolar cholinesterase inhibitors with high inhibitory potency on amyloid-β aggregation. *J. Med. Chem. 51*, 2027−2036.
(25) Camps, P., Formosa, X., Munoz-Torrero, D., Petrignet, J., Badia, A., and Clos, M. V. (2005) Synthesis and pharmacological evaluation of huprine-tacrine heterodimers: Subnanomolar dual binding site acetylcholinesterase inhibitors. *J. Med. Chem. 48*, 1701−1704.
(26) Munoz-Ruiz, P., Rubio, L., Garcia-Palomero, E., Dorronsoro, I., Monte-Millan, M. D., Valenzuela, R., Usan, P., Austria, C. D., Bartolini, M., Andrisano, V., Bidon-Chanal, A., Orozco, M., Luque, F. J., Medina, M., and Martinez, A. (2005) Design, synthesis, and biological evaluation of dual binding site acetylcholinesterase inhibitors: New disease-modifying agents for Alzheimer's disease. *J. Med. Chem. 48*, 7223−7233.
(27) Rodriguez-Franco, M. I., Fernandez-Bachiller, M. I., Perez, C., Hernandez-Ledesma, B., and Bartolome, B. (2006) Novel tacrine-melatonin hybrids as dual-acting drugs for Alzheimer disease, with improved acetylcholinesterase inhibitory and antioxidant properties. *J. Med. Chem. 49*, 459−462.
(28) Decker, M. (2006) Homobivalent quinazolinimines as novel nanomolar inhibitors of cholinesterase with dirigible selectivity toward butyrylcholinesterase. *J. Med. Chem. 49*, 5411−5413.
(29) Elsinghorst, P. W., Cieslik, J. S., Mohr, K., Trankle, C., and Gutschow, M. (2007) First gallamine-tacrine hybrid: design and characterization at cholinesterase and the M2 muscarinic receptor. *J. Med. Chem. 50*, 5685−5695.
(30) Greig, N. H., Utsuki, T., Ingram, D. K., Wang, Y., Pepeu, G., Scali, C., Yu, Q. S., Mamczarz, J., Holloway, H. W., Giordano, T., Chen, D., Furukawa, K., Sambamurti, K., Brossi, A., and Lahiri, D. K. (2005) Selective butyrylcholinesterase inhibition elevates brain acetylcholine, arguments learning and lowers Alzheimer beta-amyloid peptide in rodent. *Proc. Natl. Acad. Sci. U.S.A. 102*, 17213−17218.
(31) Carolan, C. G., Dillon, G. P., Khan, D., Ryder, S. A., Gaynor, J. M., Reidy, S., Marquez, J. F., Jones, M., Holland, V., and Gilmer, J. F. (2009) Isosorbide-2-benzyl carbamate-5-salicylate, a peripheral anionic site binding subnanomolar selective butyrylcholinesterase inhibitor. *J. Med. Chem. 53*, 1190−1199.
(32) Ellman, C. L., Courtney, K. D., Andres, V. J., and Featherstone, R. M. (1961) A new rapid colorimetric determination of acetylcholinesterase activity. *Biochem. Pharmacol. 7*, 88−95.
(33) Simons, J.-W.F.A., Boots, J. A., Kats, M. P., Slotboom, A. J., Egmond, M. R., and Verheij, H. M. (1997) Dissecting the catalytic mechanism of *Staphylococcal* lipases using carbamate substrates: Chain length selectivity, interfacial activation, and cofactor dependence. *Biochemistry 36*, 14539−14550.
(34) Shen, T., Tai, K., Henchman, R. H., and McCammon, J. A. (2002) Molecular Dynamics of Acetylcholinesterase. *Acc. Chem. Res. 35*, 332−340.
(35) Goodsell, D. S., and Olson, A. J. (1990) Automated docking of substrates to proteins by simulated annealing. *Proteins 8*, 195−202.
(36) Goodsell, D. S., Lauble, H., Stout, C. D., and Olson, A. J. (1993) Automated docking in crystallography: Analysis of the substrates of aconitase. *Proteins 17*, 1−10.
(37) Goodsell, D. S., Morris, G. M., and Olson, A. J. (1996) Docking of flexible ligands. Applications of AutoDock. *J. Mol. Recognit. 9*, 1−5.
(38) Pettersen, E. F., Goddard, T. D., Huang, C. C., Couch, G. S., Greenblatt, D. M., Meng, E. C., and Ferrin, T. E. (2004) UCSF Chimera—A visualization system for exploratory research and analysis. *J. Comput. Chem. 25*, 1605−1612.
(39) Piazzi, L., Rampa, A., Bisi, A., Gobbi, S., Belluti, F., Cavalli, A., Bartolini, M., Andrisano, V., Valenti, P., and Recanatini, M. (2003) 3-(4-{[Benzyl(methyl)amino] methyl}-phenyl)-6,7-dimethoxy-2H-2-chromenone (AP2238) inhibits both acetylcholinesterase and acetylcholinesterase-induced β-amyloid aggregation: A dual function lead for Alzheimer's disease therapy. *J. Med. Chem. 46*, 2279−2282.
(40) Leo, A., Hansch, C., and Elkins, D. (1971) Partition coefficients and their uses. *Chem. Rev. 71*, 525−616.
(41) Fujita, T., Iwasa, J., and Hansch, C. (1964) A new substituent constant, π, derived from partition coefficients. *J. Am. Chem. Soc. 86*, 5175−5180.
(42) Moraczewski, A., Banaszynski, L. A., From, A. M., White, C. E., and Smith, B. D. (1998) Using hydrogen bonding to control carbamate C-N rotamer equilibria. *J. Org. Chem. 63*, 7258−7262.
(43) Bartolucci, C., Perola, E., Cellai, L., Brufani, M., and Lamba, D. (1999) Back door opening implied by the crystal structure of a carbamoylated acetylcholinesterase. *Biochemistry 38*, 5714−5719.

(44) Carletti, E., Colletier, J.-P., Dupeux, F., Trovaslet, M., Masson, P., and Nachon, F. (2010) Structural evidence that human acetylcholinesterase inhibited by tabun ages through O-dealkylation. *J. Med. Chem. 53*, 4002−4008.
(45) Dvir, H., Silman, I., Harel, M., Rosenberry, T. L., and Sussman, J. L. (2010) Acetylcholinesterase: From 3D structure to function. *Chem.-Biol. Interact. 187*, 10−22.